Using Bioengineering Approaches to Generate a Three-Dimensional (3D) Human Pluripotent Stem Cell (hPSC)-Based Model for Neurodegenerative Diseases

By

Francis Petty

A Thesis Presented in Partial Fulfillment

of the Requirements for the Degree

Master of Science

Approved April 2016 by the

Graduate Supervisory Committee:

David Brafman, Chair

Sarah Stabenfeldt

Mehdi Nikkhah

ARIZONA STATE UNIVERSITY

May 2016

ABSTRACT

The pathophysiology of neurodegenerative diseases, such as Alzheimer's disease (AD), remain difficult to ascertain in part because animal models fail to fully recapitulate the complex pathophysiology of these diseases. In vitro models of neurodegenerative diseases generated with patient derived human induced pluripotent stem cells (hiPSCs) and human embryonic stem cells (hESCs) could provide new insight into disease mechanisms. Although protocols to differentiate hiPSCs and hESCs to neurons have been established, standard practice relies on two dimensional (2D) cell culture systems, which do not accurately mimic the complexity and architecture of the in vivo brain microenvironment.

I have developed protocols to generate 3D cultures of neurons from hiPSCs and hESCs, to provide more accurate models of AD. In the first protocol, hiPSC-derived neural progenitor cells (hNPCs) are plated in a suspension of Matrigel™ prior to terminal differentiation of neurons. In the second protocol, hiPSCs are forced into aggregates called embryoid bodies (EBs) in suspension culture and subsequently directed to the neural lineage through dual SMAD inhibition. Culture conditions are then changed to expand putative hNPC populations and finally differentiated to neuronal spheroids through activation of the tyrosine kinase pathway. The gene expression profiles of the 3D hiPSC-derived neural cultures were compared to fetal brain RNA. Our analysis has revealed that 3D neuronal cultures express high levels of mature pan-neuronal markers (e.g. MAP2, β3T) and neural transmitter subtype specific markers. The 3D neuronal spheroids also showed signs of neural patterning, similar to that observed during

embryonic development. These 3D culture systems should provide a platform to probe disease mechanisms of AD and enable to generation of more advanced therapeutics.

ACKNOWLEDGMENTS

I would like to first start out by thanking Dr. Brafman and Josh Cutts, both of whom have been instrumental in sparking my interest in the exciting field of human pluripotent stem cell research. Through their efforts, and the efforts of Dr. Stabenfeldt and Dr. Nikkhah, I have learned much in an area of research I never thought I would have been involved with. I would also like to thank Dr. Brafman and Josh for their guidance through my last years at Arizona State University.

I would also like to thank all those who have been in the Brafman lab with me during my year and a half there. Due to many of their efforts, in particular Josh Cutts, I have learned what it means to work in a lab and to conduct scientific research. I have many fond memories of those who I have worked with that I will always treasure into the future.

Finally, I would like to thank my family and friends who supported me throughout all this time. Thank you too my parents for always being supportive of me and helping me out in many different ways. Thank you to my friends for always encouraging me and pushing me forwards.

TABLE OF CONTENTS

Page

CHAPTER Page

LIST OF FIGURES

Figure Page

CHAPTER 1: Introduction

1.1 Motivation

Dementia caused by neurodegenerative diseases affects over five million Americans, costing $604 billion in care and treatment (Prince et al, 2013). These numbers are expected to significantly increase in correlation to the average age of the population. ("Brain Disorder: By the Numbers"). Due to the limited understanding of the complex pathophysiology of these diseases a curative treatment remains currently out of reach. *In vitro* disease modeling using patient derived human induced pluripotent stem cells (hiPSCs) has the potential to elucidate the mechanisms behind these diseases which then would allow for the development of a cure. It is therefore imperative any model used recapitulates the complex mechanisms inherent to the disease of interest.

1.2 Neurodegenerative Diseases

There are many neurodegenerative diseases affecting numerous regions of the peripheral and central nervous system each leading to the degradation and loss of function of their respective regions. Among these diseases there are some common pathological features, the most prominent being the aggregation of various proteins. Alzheimer's disease, Parkinson's disease, amyotrophic lateral sclerosis, and Huntington's disease all have the formation of these aggregates (Kopito, 2010).

1.2.1 Alzheimer's Disease

Alzheimer's disease (AD) affects over 5 million Americans, with a new case developing every 67 seconds and is the 6th leading cause of death (Prince et al, 2013). AD

is associated with memory loss, confusion, agitation, and depression. This makes it a tremendous burden both societally and economically for those who must provide support (Camille, Conor and Amelia, 2015). There are two main types of AD: early on set AD (EOAD) which has a known genetic component and late onset AD (LOAD) which remains sporadic. The exact mechanisms driving AD remains unknown. However, there are mutations in the amyloid precursor protein (APP), preseinilin-1 (PSEN-1) and preseinilin-2 (PSEN-2) that are thought to be key contributing factors in the production of beta-amyloid (Aβ) plaques, a pathological hallmark of AD (Tishcha, Esther and Bart, 2004). The leading hypothesis is that the Aβ plaques then cause the formation of neurofibrillary tangles (NFTs), the second pathological hallmark of AD (Oddo, Caccamo and Sheperd, 2003; Karran, Mercken, and De Strooper, 2011; Castellani, Rolston and Smith 2010). Through the use of *in vitro* modeling, AD's etiology has started to be identified (Desbordes, Lorenz, 2013). However, there is much more to learn before an effective cure can be found.

1.2.2 Parkinson's Disease

Parkinson's disease (PD) is one of the most prevalent neurodegenerative diseases second only to AD (Yarnall, Archibald and Burn, 2012). It is characterized by a progressive loss of dopaminergic neurons within the substantia nigra of the mid-brain (Wu and Hallett, 2013). Similar to AD, there are a few genetic mutations that have been shown to cause PD, but a vast majority are idiopathic. Currently there are 26 distinct chromosomal regions associated with PD and six mutations that are monogenic: SNCA, LRRK2, *Parkin*, PINK1, DJ-1, and ATP13A2 (Klein and Westenberger, 2012). Through various mechanisms all these mutations lead to the eventual progressive loss of

dopaminergic neurons. Here, again, there is the common pathological feature of protein aggregation. When specific mutations occur α-synuclein, a protein found in the presynaptic terminal, aggregates inside the neuron leading to the formation of Lewy bodies (LBs) (Figure 1-2). The formation of LBs cause a disruption in the cell through the displacement of cellular components eventually leading to cell death (Klein and Westenberger, 2012; Moore et al, 2005).

There are several dopaminergic drugs currently available for the symptomatic treatment of PD including: pramipexole and ropinirole, which show remarkable results (Schapira, 2009). However, there is no curative treatment for PD, and many of these drugs can cause dramatic neuropsychiatric symptoms further decreasing a PD patient's standard of living (Aarons, Peisah and Wijeratne, 2012). Apart from pharmacological drugs, hPSC therapy replacement has shown promise in the past as a curative treatment to PD. Human fetal ventral mesencephalic stem cells were shown to have varying results when transplanted into the striata of a PD patient's brain. Many patients saw a dramatic improvement in symptoms (Politis and Lindvall, 2012). Even with these improvements and treatments, several questions remain about PD.

1.2.3 Amyotrophic Lateral Sclerosis

Amyotrophic lateral sclerosis (ALS) is pathologically characterized by the progressive degeneration of upper and lower motor neurons. While this disease is not as prevalent as some other neurodegenerative diseases, only affecting 1 in 100,000, it is very lethal, killing those who have it 2-5 years after symptoms appear (Andrews, 2009). Similar to the other forms of neurodegenerative diseases, the cause of ALS is mostly sporadic (Aggarwal and Shashiraj, 2006). Of the familial cases, there are 16 genetic mutations that

are known to play a role in the development of ALS (Pratt, Getzoff and Perry, 2012). In the common form of familial ALS, the transcription factor TDP-43 escapes the nuclear envelope and forms protein aggregates in the cytoplasm of the affected motor neurons. These aggregates are toxic to the neuron leading to eventual cell death (Braak et al, 2010). The spreading of TDP-43 aggregates through axon terminals to post- and pre-synaptic neurons and leads to the progressive loss of motor control characterized by this disease (Feiler et al, 2015). In some cases ALS is accompanied by frontotemporal degeneration leading to dementia (Nakano, 2001).

The progressive loss of motor neurons leads to paralysis that eventually affects the diaphragm ending in respiratory failure (Orsini et al, 2015). This disease has a very bleak outlook for those who suffer from it. Currently there are no cures for ALS and very few palliative treatments available (Ludolph, Brettschneider and Weishaupt, 2012).

1.2.4 Huntington's Disease

Huntington's disease (HD) is a neurodegenerative disease characterized by severe motor and cognitive deficits between ages 35 to 44 (Frank, 2014). A trinucleotide repeat in the *HUNTINGTIN* gene leads to a toxic gain-of-function and cytoplasmic aggregate of the Huntingtin protein (HTT) (Kowalski et al, 2015). Symptoms of HD fall into two main categories: chorea and behavioral changes (Finkbeiner, 2011). HD is known to be nearly 100% familial with an autosomal dominant inheritance (Novak and Tabrizi, 2010). There are currently no cures available for HD and only minimal treatment options available for the chorea (Novak and Tabrizi, 2010).

1.3 Studying Neurodegenerative Diseases

The study of neurodegenerative diseases is vital to the creation of an effective treatment. Currently there are many different ways available to study these diseases: (1) the use of postmortem studies, (2) animal models, and (3) human induced pluripotent stem cells. These models have all helped in the furthering of the understanding of neurodegenerative disease pathology and treatments.

1.3.1 Postmortem Studies

Many of the techniques used to study neurodegenerative diseases do not recapitulate every aspect of the diseases pathology nor human physiology leaving large gaps in our understanding. The use of postmortem studies fills many of these gaps with the analysis of diseased individuals shortly after death. Currently these studies are the golden standard for examining the pathology of many neurodegenerative diseases (Hartmann, 2004). However, even with the benefits learning about human diseases in humans, postmortem studies are limited in scope. Many times individuals with these diseases take medications that can drastically alter their brain limiting the knowledge gained through this method (Pandey and Dwivedi, 2010). Another shortcoming of postmortem studies is their inability to reveal disease mechanisms as they unfold (Hartmann, 2004). The latter limitation is nearly impossible to circumvent and yet is most critical to the understanding of a disease.

1.3.2 Animal Models

Animal models allow for the study of disease mechanisms in ways previously unavailable. By using a variety of gene knock-out/in techniques and pharmacological agents many neurodegenerative diseases are, in part, able to be modeled (Simmons, 2008;

Blandini and Armentero, 2012). However, animal models have a few inherent limitations that prevent the in-depth study of neurodegenerative diseases as they appear in humans.

For an animal model to recapitulate the disease as it appears in a human its genome must be edited in highly specific ways. As stated earlier, many of the causes of neurodegenerative diseases remain elusive. This limits the ability of these diseases to be modeled using animals. In many cases the only neurodegenerative diseases being investigated in animals are the familial versions with known genetic causes (LaFerla and Green, 2012). While there have been attempts to study sporadic causes, it remains to be seen as a viable method, limiting its usefulness in the analysis of many disease (Fisher et al, 2009).

When a neurodegenerative disease is modeled in an animal there remain many significant short comings. In many cases the disease being modeled does not completely recapitulate the disease as it is seen in humans. For example, when AD is modeled in mice the formation of NFTs does not take place as it does in humans with AD (LaFrela and Green, 2012). For a model to be successful and worth studying it should have "similar symptom manifestations, similar underlying biology, [and] similar response to clinically effective therapeutic agents" (Mcgonigle and Ruggeri, 2014). However, this is not seen in many of the animal models currently being studied.

1.3.3 Human Induced Pluripotent Stem Cells

Human induced pluripotent stem cells (hiPSCs) are derived from the reprogramming of somatic cells by overexpression of the transcription factors: Klf4, c-Myc, Oct3/4, Sox2 (Takahashi et al, 2007). Once reprogrammed into hiPSCs they can then be expanded indefinitely in culture and differentiated into any somatic cell type. These characteristics

allow for many possible uses ranging from drug discovery, cell replacement therapies, disease modeling, and many more (figure 1-3). Reprogramming somatic cells from sporadic, familial, and healthy individuals and then differentiating those into the diseased cell types opens many avenues for the study of these diseases. This process can be used to compare genetic differences, mechanism, onset, and progression of the disease (Sternecket, Reinhardt and Schöler, 2014). However there is a key limiting factor when using hiPSCs, or any cells, *in vitro* to study diseases: the ability for the *in vitro* culture to recapitulate the complex pathology and pathophysiology inherent to the disease and the affected tissue.

1.3.3.1 *In Vitro* Two-Dimensional Disease Modeling Systems

A common method of studying diseases is differentiating and examining hiPSCs on the surface of tissue culture. However, due to the simplistic nature inherent to two-dimensional (2-D) models many aspects of the native cell environment is loss (Sung et al, 2013). It has been shown that many key pathological hallmarks of neurodegenerative diseases, such as the formation of Aβ plaques and NFTs characteristic of AD, do not form in these 2-D culture systems (Benam et al, 2015).

1.3.3.2 *In Vitro* Three-Dimensional Organoid Systems

To further emulate the complex microenvironments of organs there a focus on three-dimensional (3-D) systems. 3-D systems have been used for the study of almost every organ of the body, showing increased functionality and structure organization over their 2-D counterparts (Huch and Koo, 2015). This has led many to hypothesize that 3-D models will be able to recapitulate disease pathology in a more accurate manner than previously studied (Noble and Burns, 2010).

1.4 Overall Goal

The need for an *in vitro* system that accurately models neurodegenerative diseases is crucial to further the understanding of the complex pathophysiology of these diseases. **Chapter 2** describes the development of two assays used in the validation of hPSC differentiation strategies. **Chapter 3** describes the development of 3-DhPSC differentiation protocols to allow for the generation of neuronal cells *in vitro*. **Chapter 4** describes the development of methods and protocols for the generation of ventricular cardiomyocytes from hPSCs. **Chapter 5** summarizes my research and provides some future directions for the protocols developed.

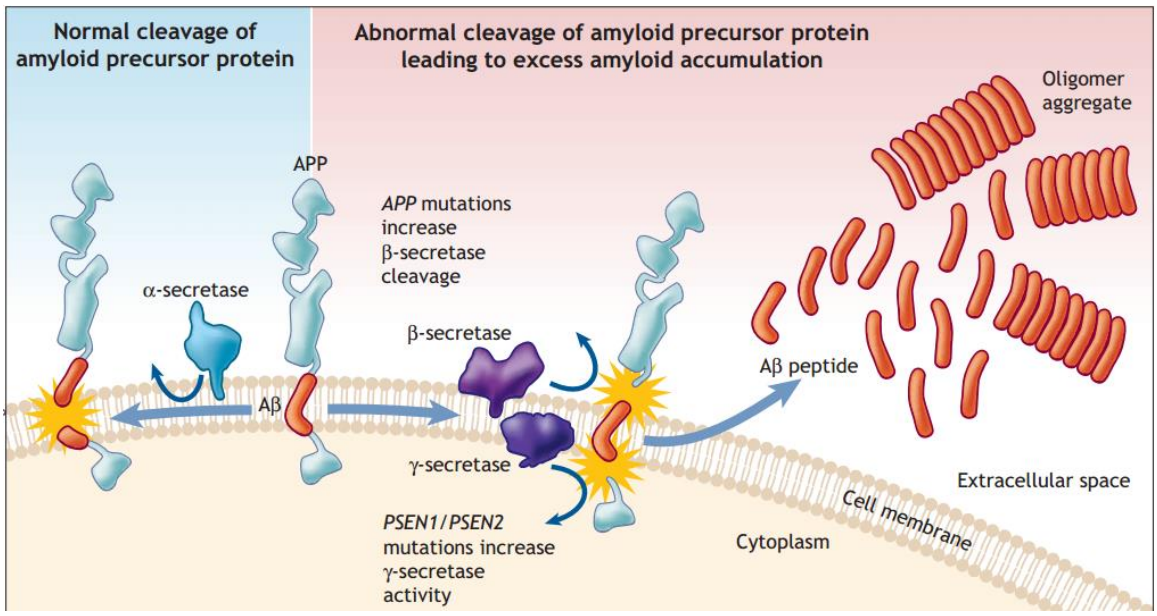

Figure 1-1: Comparison of Normal and Diseased Cleavage of Aβ in Alzheimer's Disease

Alzheimer's disease is characterized by the formation of amyloid-beta plaques. In healthy individuals α-secretase cleaves APP in its transmembrane segment preventing the production of Aβ. In AD patients β- and γ-secretase cleave APP at the terminal ends of Aβ allowing its release and aggregation in the extracellular space (Patterson et al, 2008).

Chapter 2: Development of Assays to Evaluate Neuronal Differentiation of hPSCs.

2.1 Introduction

During the differentiation of hPSCs to mature cells, many morphological changes take place. It is difficult to analyze cells based purely on morphology, and so a more robust, quantifiable method is required. Measuring gene expression through reverse transcriptase – quantitative polymerase chain reaction (RT-qPCR) has been proven as one of the most useful techniques available to measure gene expression of cells (Marino et al, 2003). Using this technique, relative changes in gene expression can be compared across several conditions.

For my research RT-qPCR was the main method used in the evaluation of 3-D and 2-D hPSC differentiation methods. Here, I have developed a panel of RT-qPCR primers that were used for the analysis of the 2-D and 3-D neuronal differentiation techniques discussed in chapter 3 (figure 2-1).

2.2 Primer Design

I initially sought to identify genes expressed in the desired differentiated cell types (Figure 2-1A). For 2-D and 3-D neuronal differentiation methods I needed to be able to examine the changes in gene expression as the hPSCs differentiated into the neuronal lineage (figure 2-2). The four primary cell types which required analysis for this protocol are: NPC, general glial, general neural, and neuronal subtype.

In designing primers corresponding to these specific targets, NCBI Primer-BLAST was utilized (Figure 2-1B) (Ye et al, 2012). I evaluated three criteria in the design of the primers: primer length, product length, and primers spanning exon-exon junctions. Primer length is crucial for the specificity of RT-qPCR product amplification. If the primer is too long, specificity will be ensured. However, amplification efficiency will greatly reduced, therefore skewing the data collected. If the primer is too short, specificity will be loss and off target binding will occur. Therefore, I designed primers to be 18-24 nucleotides which has been found to be ideal for RT-qPCR (Real-Time PCR Handbook). Various methods exist in the detection of RT-qPCR products, for this project SYBR Green DNA binding dye was utilized. SYBR Green DNA binding dye is a molecule which fluoresces when bound to double stranded DNA (dsDNA), the product of RT-qPCR. Product length was designed around SYBR Green DNA binding dye, which has an optimal product length of 50-200 bp long (Real-Time PCR Handbook). When possible, I designed all primers to span an exon-exon junction. Primers designed in this way are unable to bind to genomic DNA that may not have been purified out during RNA isolation.

2.3 Testing and Validation

Before the primers can be used for experimental purposes, they must be tested to confirm their specificity. This was done by running RT-qPCR with the primers on primary tissue samples that have been previously verified to have high expression of the target gene (Figure 2-1C). Therefore, these primers were verified against RNA extracted from fetal brain tissue weeks 20-26 (CloneTech). Once amplification of the target gene is

confirmed, via RT-qPCR, the primers are then validated for target specificity. Two methods are used in tandem to confirm this: melt curve and agarose gel electrophoresis (Figure 2-1D).

A melt curve is generated as the last step in RT-qPCR. The concept of a melt curve is that the DNA denaturing temperature is highly specific to its length and composition. To generate a melt curve, at the end of an RT-qPCR analysis, the thermocycler will slowly increase the temperature. As the DNA starts to denature, the SYBR Green DNA binding dye will unbind from the DNA, change in fluoresce is then measured with respect to time. If the primer is specific, a single melt peak is to be expected as all the dsDNA should denature at the same temperature (Figure 2-3A). If, however, the primer is not specific, there will be two or more melt peaks (Figure 2-3B).

It is possible for an off target amplification to occur that is of similar denaturing temperature as the target gene. In this instance the melt curve would be obscured by the target gene melt curve, and thus have the appearance of only a single product. To further confirm the primers are specific, I used agarose gel electrophoresis to separate the products amplified during RT-qPCR based on size. If after using this method there is only a single band the primer is then considered validated and stored for future use. However, if there are two bands then the primer is not specific (Figure 2-4) and must be redesigned. This is an iterative process that will be repeated until all the primers are completed.

I designed primers RT-qPCR primers for the comparison neuronal differentiation of hPSCs for in a 2-D and 3-D environment. These primers were tested against RNA

isolated from fetal brain and were validated for specificity. The complete list of developed primers can be found in appendix A.

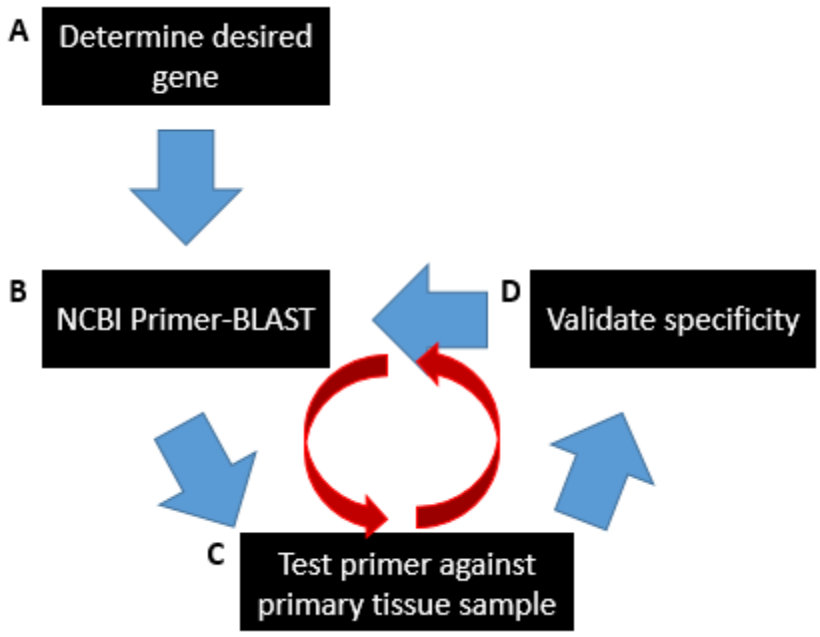

Figure 2-1: RT-qPCR Primer Development Process

The Iterative process required for the design of RT-qPCR primers.

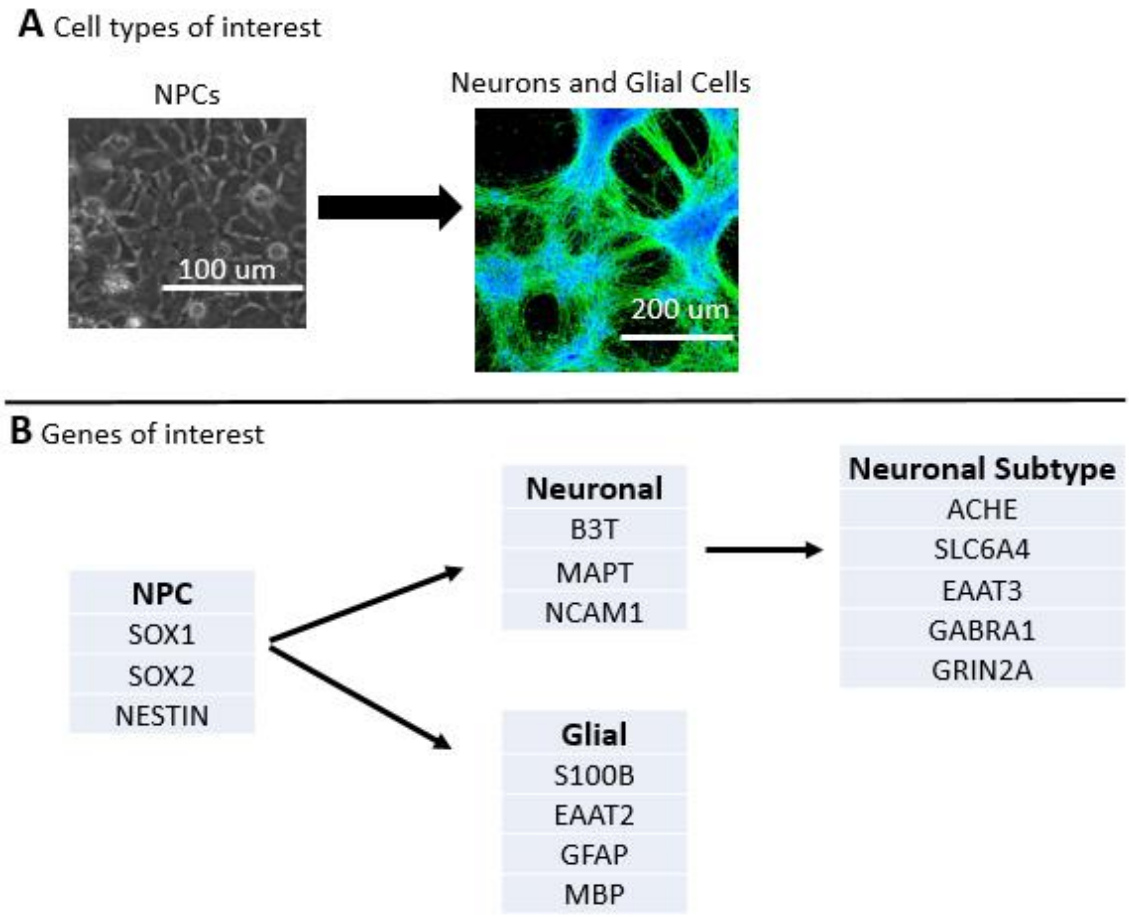

Figure 2-2: Identification of Neuronal Genes

(A) An examination of the neuronal differentiation protocols revealed three main cell types: NPCs, neurons, and glial cells. (B) Genes specific to these cell types were researched and the panel of primer targets was established.

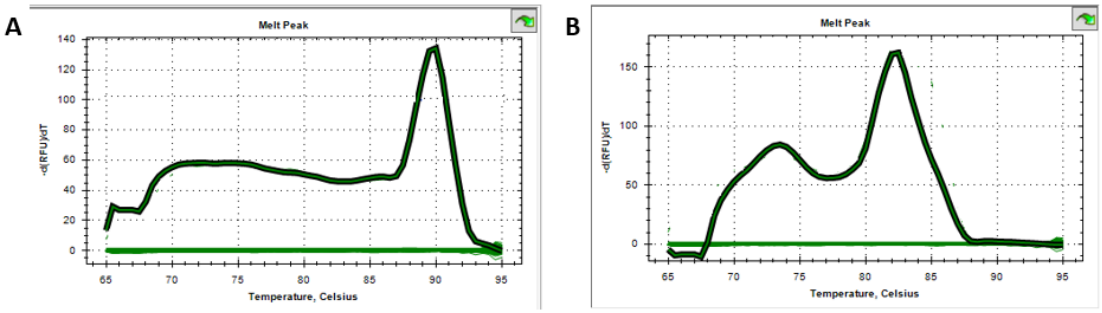

Figure 2-3: Melt Peaks from RT-qPCR

(A) A single melt peak is present, suggesting a single PCR product. (B) Two distinct peaks are present, indicating the primer was not specific, allowing for the amplification of two products. X-axis is temperature in Celsius and Y-axis is the inverse in the change of fluorescence with respect to time.

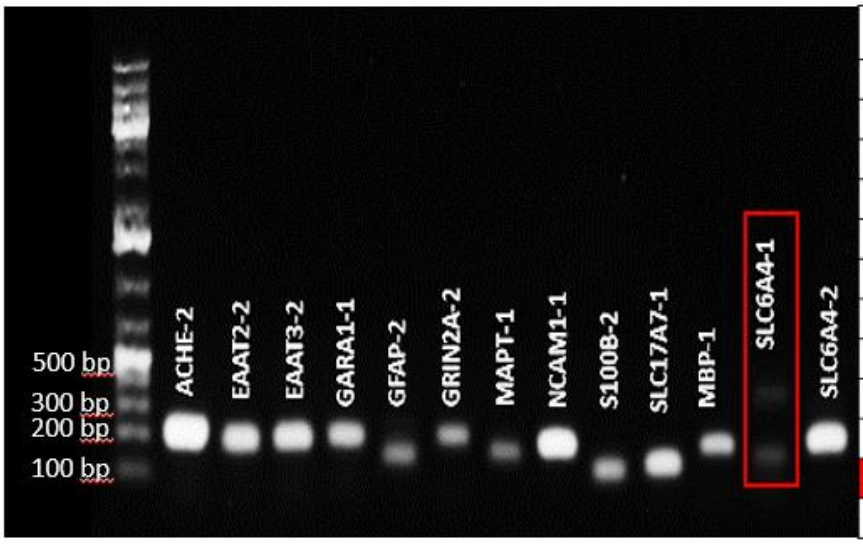

Gene	Product Length (bp)
ACHE-2	188
EAAT2-2	172
EAAT3-2	181
GABRA1-1	194
GFAP-2	128
GRIN2A-2	191
MAPT-1	140
NCAM1-1	178
SLC17A7-1	116
MBP-1	175
SLC6A4-1	140
SLC6A4-2	144

Figure 2-4: Agarose Gel Electrophoresis

A sample of an agarose gel with the RT-qPCR products for validation. Most channels only have a single band indicating the primers were specific. SLC6A4-1, boxed in red, has two bands proving it is not specific.

CHAPTER 3: Development of 3-D Neuronal Differentiation

3.1 Abstract

The pathophysiology of neurodegenerative diseases remains difficult to ascertain in part, because current models fail to fully recapitulate the complex pathophysiology associated with them. *In vitro* models of neurodegenerative diseases generated with patient derived human induced pluripotent stem cells (hiPSCs) could provide new insight into disease mechanisms. Although protocols to differentiate hiPSCs to neurons have been established, standard practice relies on two-dimensional (2-D) cell culture systems, which do not accurately mimic the complexity and architecture of the *in vivo* microenvironment. I have developed and evaluated protocols that allows for the three-dimensional (3-D) neuronal differentiation of hiPSCs which have the potential to be further developed into neurodegenerative disease models.

3.2 Introduction

Currently in the United States there are more than 6 million individuals suffering from a neurodegenerative disease. The cost of treatment and care for these people is more than $600 billion (Brain Disorder by the numbers). For many neurodegenerative diseases the pathophysiology is incredibly complex and exceedingly difficult to study. There have been many different techniques used to learn about the mechanisms behind these disease: postmortem studies, animal models, and two-dimensional (2-D) human induced pluripotent stem cell models. However, none of these have shown the ability to accurately recapitulate the pathology of these complex and devastating diseases. Therefore, there has been a shift into the research of three-dimensional (3-D) organoid

models that have proven to provide a more accurate model of a variety of disease (Huch et al, 2015). Here, I develop and evaluated protocols that allows for the 3-D neuronal differentiation of human pluripotent stem cells (hPSCs). Specifically, I evaluated the following protocols: using Matrigel™ as a support structure for neuronal differentiation, with both (1) thick and (2) thin gel structures, (3) and performing neuronal differentiation on 3-D cell aggregates form human neuronal spheroids (hNS).

3.3 Materials and Methods

3.3.1 Medias

3.3.1.1 Essential 8 (E8)

E8 is a xeno-free, defined maintenance media used for the long term expansion of hPSCs. DMEM/F12 is used as a base supplemented with: sodium bicarbonate, L-Ascorbic acid-2-phosphate, sodium selenite, transferring, insulin, FGF2, TGFB, and penicillin streptomycin.

3.3.1.2 Neural Media

Neural base media (NBM) is composed of DMEM/F12 supplemented with 0.5% N2, 0.5% B27 and 1% GlutaMAX. This is used as a base media for the following neuronal differentiation media.

Neural induction media (NIM): 200 ng/ml Noggin (NOG) and 0.5 uM Dorsomorphin (DM)

Neural expansion media (NEM): 20 ng/ml basic fibroblast growth factor (bFGF) and 20 ng/ml epidermal growth factor (EGF)

Neural differentiation media (NDM): 20 ng/ml brain-derived neurotrophic factor (BDNF), 20 ng/ml glial derived neurotrophic factor (GDNF), 0.5 uM dibutyrl-cAMP (db-cAMP), and 20 ng/ml DAPT, a Notch inhibitor.

Human neuronal spheroid media (hNSM): 20 ng/ml brain-derived neurotrophic factor (BDNF), 20 ng/ml glial derived neurotrophic factor (GDNF)

3.3.2 Maintenance of Neural Progenitor Cells and HPSCs

HPSCs were expanded and maintained in an undifferentiated state at standard conditions (37^{o}C, 5% CO_2) on Matrigel™ coated polystyrene tissue culture plates. E8 media was changed every day. Cells were allowed to grow till 70-80% confluency and were passed at 2 x 10^4 cells/cm^2, every three to four days as required.

Neural progenitor cells (NPCs) were expanded and maintained on poly-L-ornithine and Laminin (PLO/LN) coated plates. They were cultured in NEM which was changed on days one and three. Once cells were 100% confluent they were passaged to a new PLO/LN coated plate at 1.2 x 10^4 cells/cm^2, every three to four days as required.

3.3.3 2-D Neuronal Differentiation of hPSCs

Figure 3-1 shows the outline of the 2-D neuronal differentiation protocol. HPSCs were grown on Matrigel™ and dissociated using Accutase once they reached 80% confluency. They were then suspended in 3 ml NIM and 5 mM ROCKi in a 6-well ultra-low adhesion plate at a concentration of 2 x 10^6 per well and placed on a shaker at 95 RPM in the incubator. After one day cells aggregated forming embryoid bodies (EBs). Half the media was changed each day. After five days, EBs were transferred to Matrigel™ coated plates and allowed to adhere for two days in NIM. After two days the

media was changed daily with NIM. After seven days neural rosettes that had formed were dissociated using Accutase and re-plated on PLO/LN coated plates in NEM and 5 uM ROCKi. After three passages only NPCs were present and were maintained or expanded as needed. To further differentiate NPCs to neurons they were grown to 100% confluency and then media was replaced with NDM. Half of the NDM was then changed daily for two weeks, at which time cells were analyzed using immunofluorescence (IF) and RT-qPCR (Brafman, 2014).

3.3.4 3-D Differentiation of hESCs to Neurons

3.3.4.1 Thick 3-D Matrigel™ culturing

NPCs were maintained on PLO/LN coated plates, in standard conditions until they were 100% confluent. Cells were incubated in Accutase for 6-7 minutes and were then suspended in cold NDM and counted. The cells were then diluted to a 1:1 concentration of Matrigel™ and cell/NDM mixture for a final concentration of 8 x 10^6 cells/ml, along with 5 uM of ROCKi and vortexed for 30 seconds. A 0.4 um pore diameter ThinCert (Greiner Bio-One) was placed into a well and 300ul of the Matrigel™/cell/NDM mixture was added into the ThinCert (figure 3-2B). The plate was then incubated at standard conditions over night. The following day a gel was visible to the naked eye, and multiple cell planes were confirmed using a microscope. 1.4 ml of NDM was added to the side of the well and 0.1 ml of NDM was gently added to the inside of the ThinCert. Half of the media was changed every day.

3.3.4.2 Thin 3-D Matrigel™ culturing

NPCs were maintained on PLO/LN coated plates in standard conditions until they were 100% confluent. Cells were incubated in Accutase for 6-7 minutes and were then

suspended in cold NDM and counted. The cells were then diluted into a 1:1 concentration of Matrigel™ and cell/NDM mixture for a final concentration of 8 x 10^6 cells/ml. Five times this volume of cold NDM was added to the solution along with 5 uM ROCKi and vortexed for 30 seconds. After, 100 ul of the Matrigel™/cell mixture was added to a 96-well plate and incubated over night at standard conditions (Figure 3-2A). The following day 200 ul of warm NDM was added to each well. Half the media was changed every day for the next four to six weeks. Extreme care was taken when removing and adding media as the gels were very fragile and peeled off the plate easily.

3.3.4.3 Human Neuronal Spheroid Differentiation

HPSCs were cultured on Matrigel™ until they reached 70-80% confluency where they were then dissociated by incubation in Accutase for 6-7 minutes. 2.0 x 10^6 cells were then suspended in ultra-low adherent tissue culture plates on a shaker (95 RPM) in standard conditions in 3ml of NIM and 5uM ROCKi. Half the media was changed every day for five days. The cells aggregated together on the first day and formed EBs. In this state the cells began differentiating down the ectodermal germ layer (Chambers et al, 2009). On day six the EBs were kept in the low adherent culture conditions and NIM was exchanged for NEM. The cells were maintained in this media for 18 days, with half the NEM changed daily. During this time the cells were proliferative and many of the EBs grew dramatically in size. On day 25, NEM was exchanged for hNSM. This media was used for the next 18 days with half the media changed daily. At this time the cells differentiated into neurons and glial cells comprising the human neuronal spheroids. On day 43 hNSM was exchanged for NBM and media was changed every 2-3 days as it turned yellow, due low pH in the presence of phenol red.

3.3.5 RT-qPCR

RT-qPCR was performed at specific time points to analyze progress of neuronal differentiation. For the 2-D cultures, cells were dissociated by incubation in Accutase for 5-7 minutes. They were then pelleted and stored at -80^{o}C. For the Matrigel™ thick 3-D cultures the gels were removed from the inserts by slitting the bottom and centrifuging for 5 minutes in a 15 ml conical tube and stored at -80^{o}C. The thin 3-D gels were removed by incubating in Accutase for 6-7 minutes and then were removed by pipetting the Accutase quickly up and down in the well. They were then pelleted and stored at -80^{o}C. RNA was isolated with a NucleoSpin™RNA kit (Macherey-Nagel) and cDNA synthesized using iScript RT Supermix (Biorad). RT-qPCR was done with iTaq Universal SYBR Green SMX 500 (Biorad) to form the master mix. RT-qPCR primers developed in chapter 3 were used. The Bio-Rad CFX384 real-time PCR detection system was used to run the RT-qPCR. Results were analyzed from the cycle threshold (CT) values using delta-delta CT method.

3.3.6 Immunofluorescence

Immunofluorescence was performed on the samples to determine the structure and protein expression of the neurons. For the 2-D cultures and thin 3-D on days 14 and 28, respectively, the cultures were washed three times with Dulbecco's phosphate-buffered saline (DPBS). Fixation buffer (BD Biosciences) was added to the wells for 15 minutes. The buffer was removed and the cultures were washed again with DPBS. Perm Buffer III (BD Biosciences) was then added to the wells for 15 minutes. The cells were washed again with DPBS and primary antibodies were add along with Hoechst and were incubated wrapped in foil at 4^{o}C overnight. The cells were washed again with DPBS and

the secondary fluorescent antibody was added for 1 hour and incubated at 37^{o}C. A final wash was done and cultures were wrapped in foil and stored at 4^{o}C.

3.3.7 Statistical Analysis

All values are shown as mean ± standard deviation. A p-value of <0.05 was considered statistically significant.

3.4 Results and Discussion

A 2-D *in vitro* environment is unable to recapitulate many facets of the cell architecture, and therefore cannot be used to study many neurodegenerative diseases. To this end, three 3-D protocols were developed and tested to allow for neuronal differentiation of hPSCs which could improve *in vitro* disease models: Matrigel™ gels, thick and thin, and suspension culture of hNS.

3.4.1 Thick and Thin 3-D Matrigel™ Culturing

To examine the viability as a 3-D neuronal differentiation system, NPCs were differentiated with NDM in Matrigel™. Matrigel's™ capability to solidify into 3-D gels and its ability to recapitulate more of the *in vivo* microenvironment, through the presence of extracellular matrix proteins and growth factors, makes it ideal for 3-D differentiation of hPSCs.

Well inserts, ThinCerts, were used for the thick 3-D gel neuronal differentiation of NPCs (Figure 3-2B). In a standard, *in vitro* environment, a cell's metabolic activity decreases the pH of their media below normal physiologic conditions. Phenol red is a pH indicator that is commonly added to media to indicate pH level by a change in media color. Over the course of one week, the media added to the thick 3-D gels no long

changed color, indicating little to no cell metabolic activity. We hypothesized that poor gas and nutrient diffusion through the thick 3-D Matrigel™ cultures resulted in high levels of cell death. This is further confirmed when an LDH assay was run on the thick 3-D samples. To find maximum LDH release, 100 ul of Triton X-100 (20% Triton X-100, 90% DPBS) was added to the ThinCert to lyse the cells and allowed to incubate for two hours. Media samples were then taken from inside of the ThinCert and the surrounding media. The LDH assay kit was then used to measure relative fluoresce. Relative fluorescence from inside the ThinCert was significantly higher than fluorescence from the surrounding media. In fact, fluorescence from the surrounding media was equivalent to that of the control, fresh media (Figure 3-3B). This discrepancy between LDH present inside and surrounding the ThinCert demonstrates the low diffusion ability of the thick 3-D gels.

Due to low diffusion, we developed a protocol in which thinner 3-D gels were employed (Figure 3-2A). However, the thin gels proved highly susceptible to mechanical disruption due to media changes, resulting in the loss of a significant amount of cultures (Figure 3-3A). The LDH assay revealed a significant amount of cell death over the first few days in culture, demonstrating that by day three a majority of cells had died (Figure 3-3D). IF staining of B3T, a general neuron marker, showed no neurite structures present in culture, illustrating the inability of thin 3-D gels to differentiate hPSCs to neuronal cells (Figure 3-1C). We hypothesize, that while cells still remained in the culture for the period of neuronal differentiation, they were dead and embedded in the Matrigel™.

A common issue with differentiation protocols, is the heterogeneity of available cell lines and their variable response to the same stimuli (Abbot et al, 2006). To this end,

three different hPSCs lines were tried: two hESCs and one hiPSCs (Figure 3-4A, B). Trials with the three cell lines gave rise to similar results with no neurite morphology and high sensitivity to mechanical disruption. Additionally two cell density gradients (1.5 x 10^5 and 1.0 x 10^5cells per well) (Figure 3-4A, B) and three Matrigel™ concentration (1:10, 1:15, 1:20) (data not shown) were tried. These two variables showed no improvement in culture survivability for both thick and thin gels.

RT-qPCR was attempted to compare gene expression of the multiple techniques. Matrigel is composed of a high quantity of RNA and proteins that are difficult to remove during RNA isolation. This resulted in high impurity of the samples during RNA isolation, preventing their analysis using RT-qPCR. Additionally, cryofixation was needed to perform IF on the thick 3-D samples. During this process, the gel was not structurally stable, forming a semi-round bead when removed from the ThinCert, preventing the investigation of its internal structure. Due to our inability to differentiate the hPSCs to neuronal cells, along with the difficulty experienced in analysis of the samples, the 3-D Matrigel™ method was abandoned.

3.2 Human Neuronal Spheroids

Nest, I developed and evaluated a suspension culture method for 3-D neuronal differentiation of hPSCs. The development of these human neuronal spheroids (hNS) took several months of experimentation with a variety of different factors including: hPSC line and cell density (Figure 3-5). Through this experimentation, I determined HUES9 TOP-GFP at 1.0 x 10^6 cells per well was the best cell line and density based cell survivability and morphology of the hNS compared to that of the other cell lines examined.

3.2.1 Gene Expression

The protocol for hNS differentiation is shown in figure 3-6A. RT-qPCR was used to measure gene expression during neuronal differentiation. Differentiation of NPCs was assessed by IF and RT-qPCR for NPC markers *SOX1*, *SOX2*, *NESTIN* (Figure 3-6B). By day 30, IF indicated the presence of NESTIN throughout hNS, confirming differentiation to NPCs from hPSCs. The Neuronal markers *MAPT*, *B3T*, and *NCAM1* were examined using RT-qPCR. Figure 3-7 shows an increase in the neuronal maturity marker *MAPT* compared to hiPSCs and similar levels of expression of all three markers as compared to the 2-D protocol by day 52 of the hNS differentiation. At day 52, neuronal subtypes were examined, demonstrating the presence of a heterogeneous neuronal population via RT-qPCR (Figure 3-8). Expression of glial cell markers were analyzed signifying the presence of cells with astroglial characteristics (Figure 3-9). Together, these results confirm that the hNS are differentiating into a heterogeneous population of neuronal cells and are currently as effective in differentiation as the 2-D protocol.

3.3 Conclusion

Multiple neuronal differentiation protocols were developed and tested in order to provide a 3-D system in which neurodegenerative diseases can be studied. We found that hPSCs suspended in a Matrigel™ gel did was as a viable means for neuronal differentiate. However, using a suspension culture technique to form hNS in suspension culture proved effective in neuronal differentiation of hPSCs in a 3-D environment. RT-qPCR results have shown that this method is equivalent to standard 2-D methods. I

hypothesize that further optimization of this protocol would allow for increased efficiency and maturity of the neuronal differentiation.

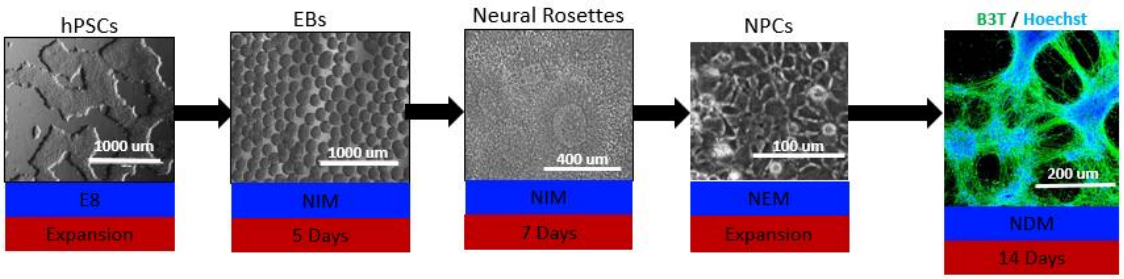

Figure 3-1: Protocol for Generation of NPCs and 2-D Neuronal Differentiation
Protocol for 2-D differentiation of hPSC to NPCs and Neuronal cells.

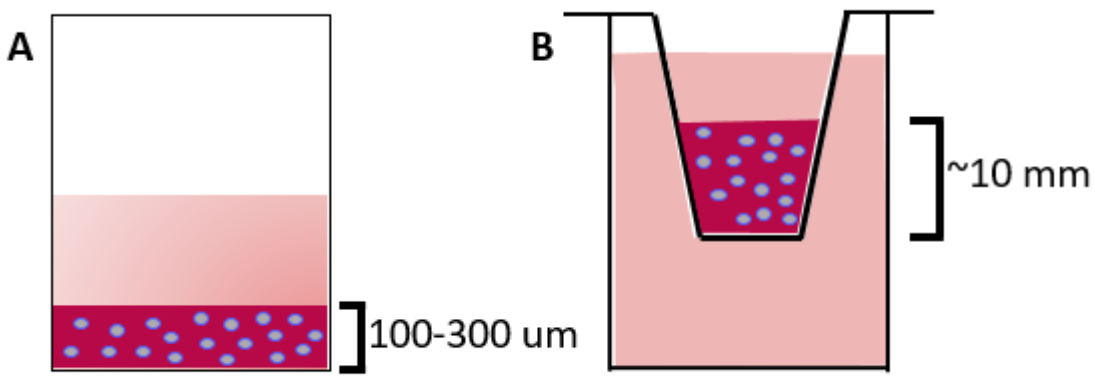

Figure 3-2: Illustration of Thick and Thin 3-D Matrigel™ Methods

(A) An illustration of the NPCs suspended in a thin 3-D Matrigel™ gel at the bottom of a well. (B) An illustration of NPCs and Matrigel™ suspended in a ThinCert for the thick 3-D neuronal differentiation.

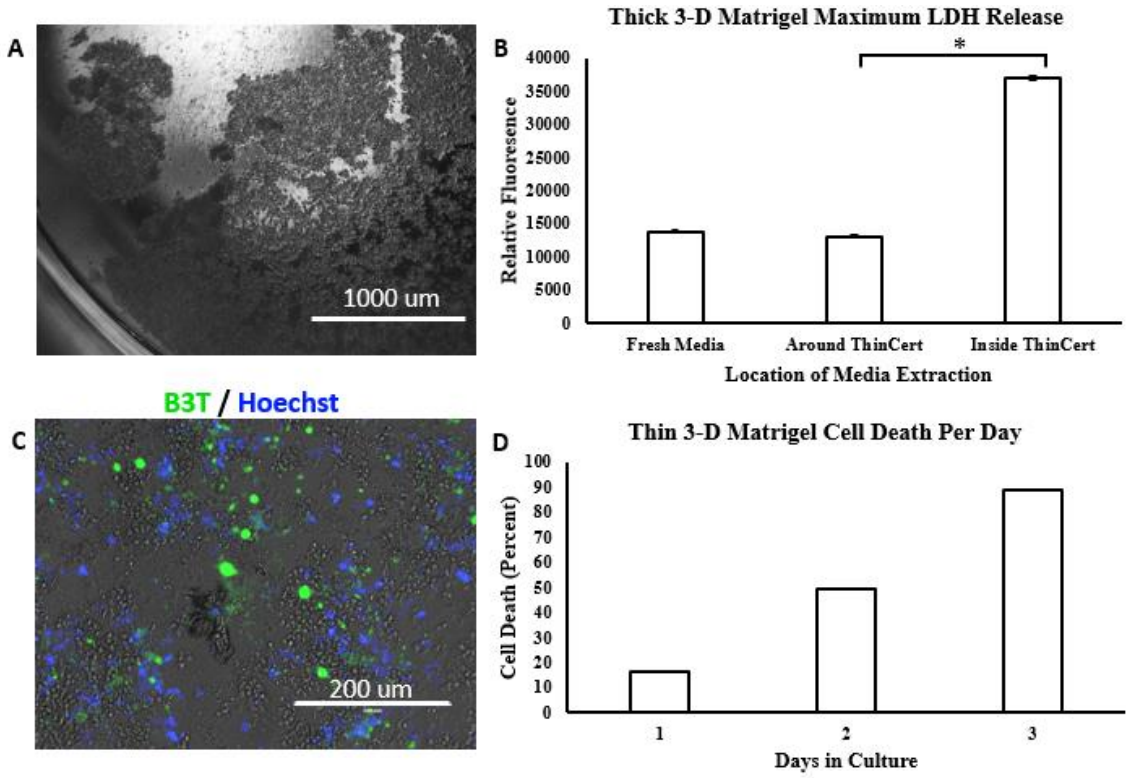

Figure 3-3: 3-D Matrigel™ Cultures Differentiation and Survivability

(A) Thin 3-D gels were highly susceptible to peeling when media was changed. Large gaps can be seen where Matrigel™ gel has detached from the plate. (B) LDH assay measuring relative fluorescence taken from media around the ThinCert compared to media taken from inside the ThinCert two hours after cell lysis. Relative fluorescence from fresh media is comparable to media taken from around the ThinCert two hours after the cells being lysed (mean ± SD of two biological samples). *P<0.05 using student's t-test). (C) IF staining of day 28 thin 3-D Matrigel™ neuronal differentiation, nuclear Hoechst (blue) and B3T (green) stained. No intact nuclei or B3T structures were observed. (D) Percent of cells that have died each day as determined by LDH assay showing increased cell death over consecutive days.

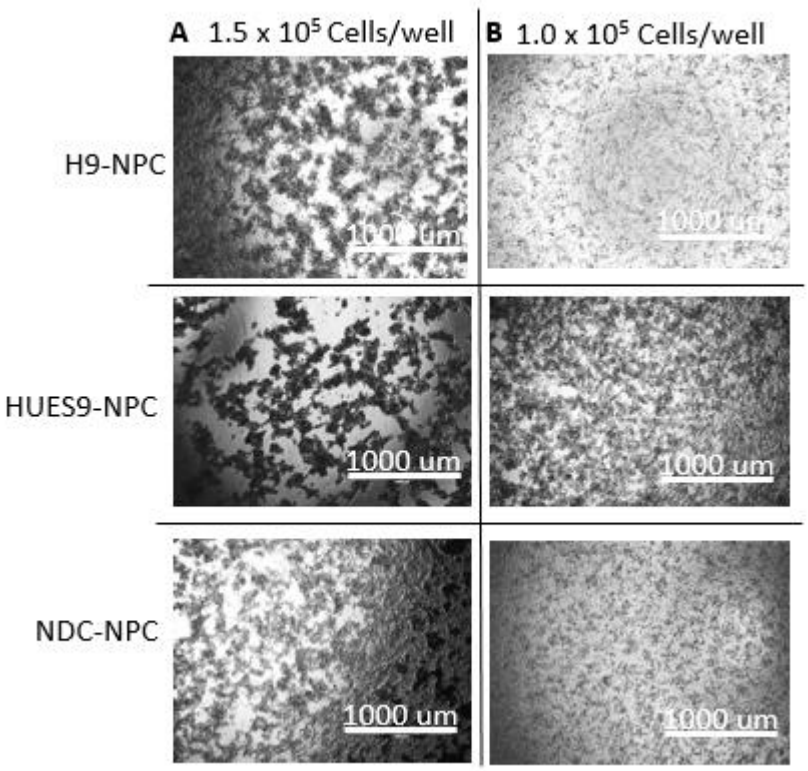

Figure 3-4: Optimization of Cell Line and Cell Density for Thin 3-D Matrigel™

Three cell lines and two densities were tested for the thin 3-D protocol. (A) With a high cell density of 1.5 x 10^5 cells per well, there was increased cell death by day seven as compared to the low density (B). The lower density condition displayed higher cells survivability for a longer period of time. However, by day ten the same peeling was present at low density as the high (data not shown).

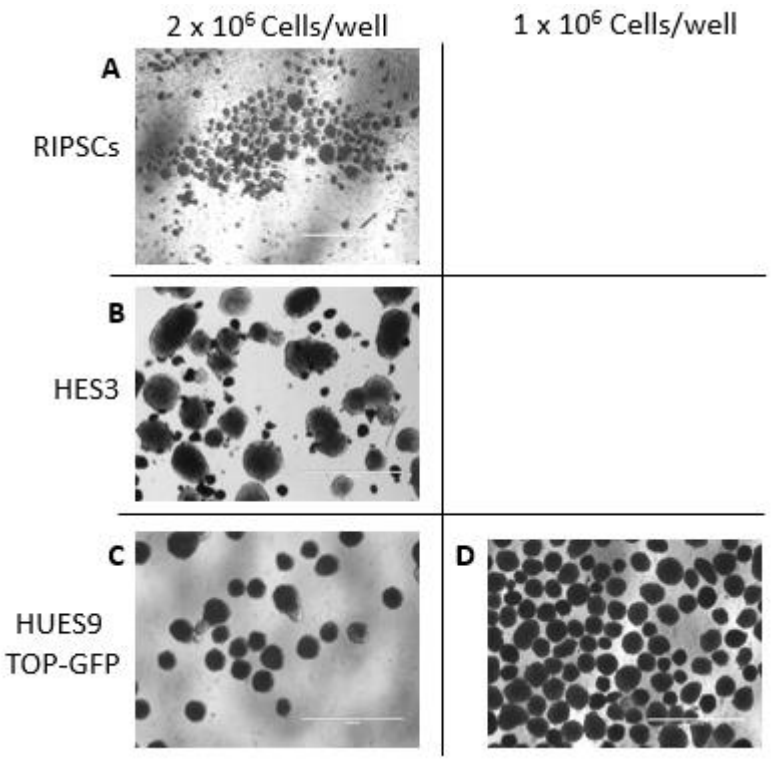

Figure 3-5: Optimization of Cell Line and Cell Density for HNS

(A) By day seven of hNS protocol cell death was extremely prevalent when using RIPSCs line. (B) HNS protocol for the HES3 cell line showed high variability when using HES3 cells, with many atypical EB morphologies. (C) Day ten of hNS protocol using HUES9 TOP-GFP demonstrated less morphological variance as well as comparatively minimal cell death. (D) HUES9 TOP-GFP was further optimized to a density of 1 x 10^6 cells per well which demonstrated increased survivability of EBs.

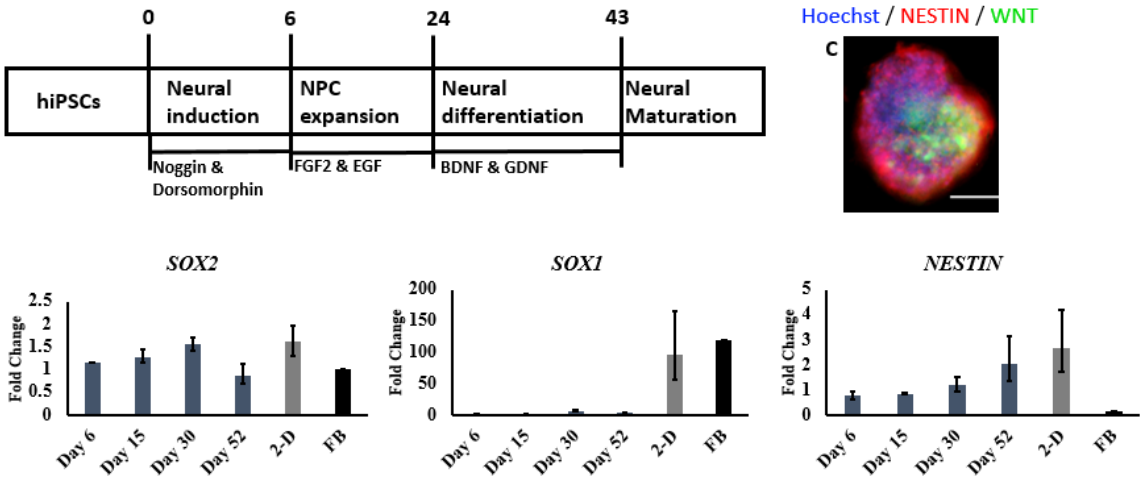

Figure 3-6: Time Course and IF of NPC Genes During hNS Differentiation

(A) Schematic of protocol for hNS differentiation. (B) Gene expression time course of NPC markers *SOX2*, *SOX1*, and *NESTIN* was determined by RT-qPCR (mean ± SD of two biological samples, normalized to 18s and relative to hiPSCs). *P < 0.05. Using ANOVA no statistical significant differences were present. This is compared to the 2-D protocol (2-D) 14 days after differentiation as well as RNA isolated from fetal brains (FB) 20-26 weeks old. (C) IF of hNS day 30, hoechst nuclear stain (blue), NPC marker NESTIN (red), and endogenous WNT (green) (scale bar = 200 um).

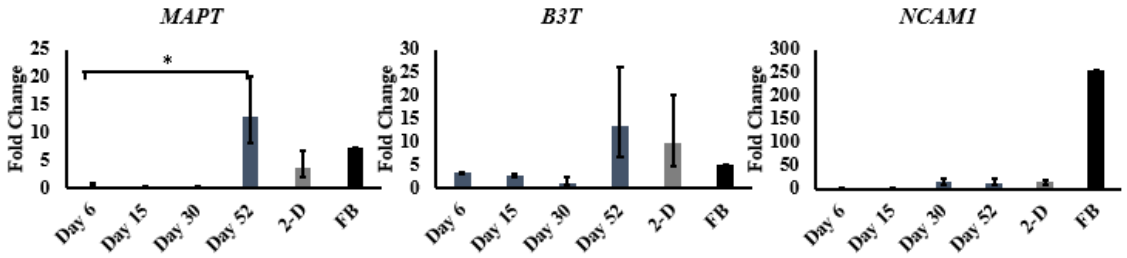

Figure 3-7: Time Course of Neuronal Specific Genes

Time course of gene expression for neuronal specific genes *MAPT*, *B3T*, and *NCAM1* were determined by RT-qPCR (mean ± SD of two biological samples, normalized to 18s and relative to hiPSCs). *P < 0.05. This is compared to the 2-D protocol (2-D) 14 days after differentiation as well as RNA isolated from fetal brains (FB) 20-26 weeks old.

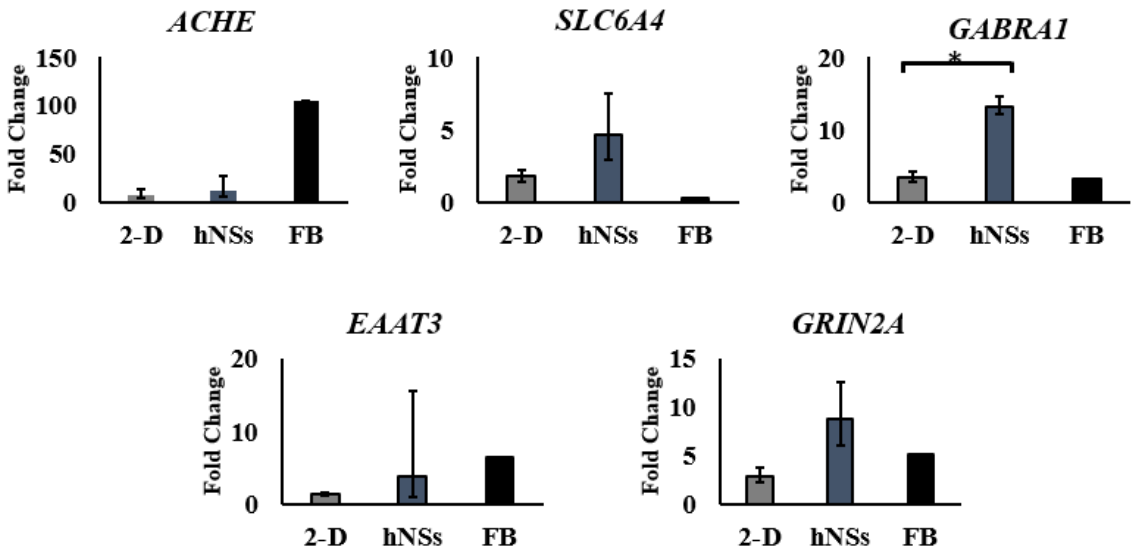

Figure 3-8: Comparison of Neuronal Subtype Gene Expression of HNS, 2-D, and FB

Measurement of neuronal subtype genes as measured by RT-qPCR (mean ± SD of two biological samples, normalized to 18s and relative to hiPSCs) for day 14 2-D, day 52 hNS, and weeks 20-26 fetal brain (FB). *$P < 0.05$ as determined by student's t-test. Similar levels of expression were found in most neuronal subtype genes for the hNS and 2-D protocols.

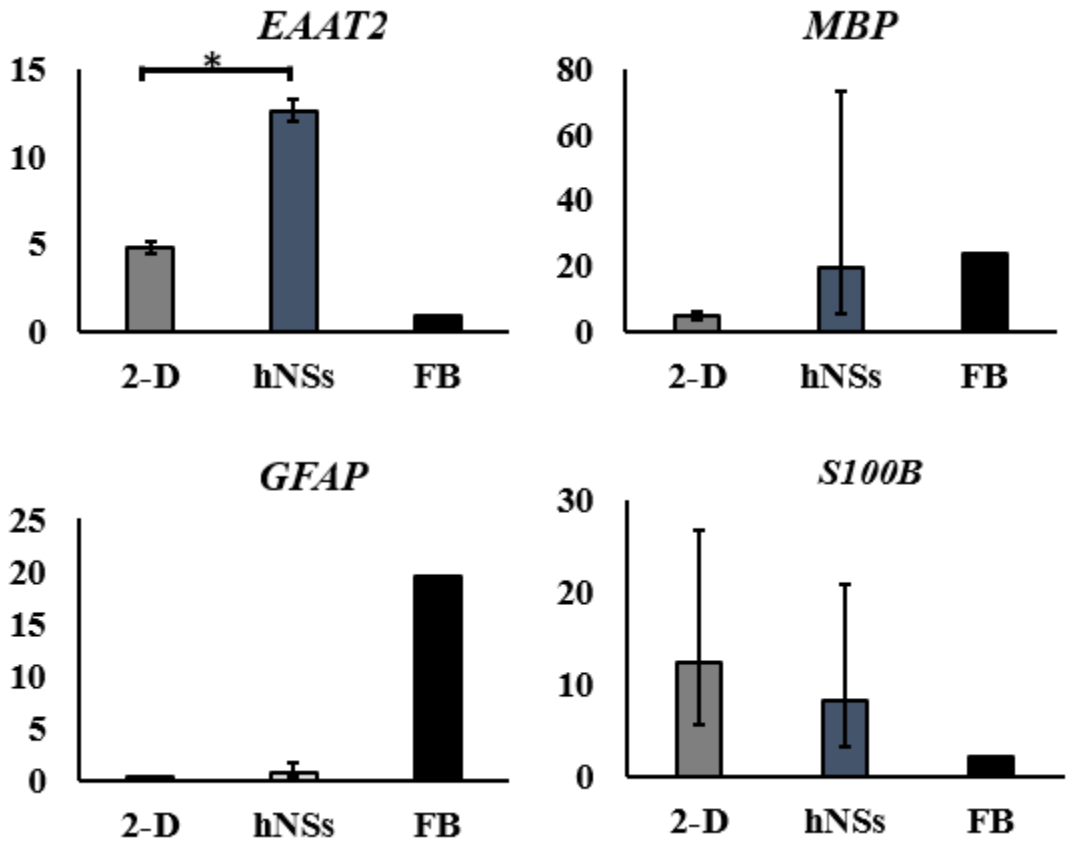

Figure 3-9: Comparison of Glial Cell Gene Expression of hNS, 2-D, and FB

Measurement of glial cell genes as measured by RT-qPCR (mean ± SD of two biological samples, normalized to 18s and relative to hiPSCs) for day 14 2-D, day 52 hNS, and weeks 20-26 fetal brain (FB). *$P < 0.05$ as determined by student's t-test. Similar levels of expression were found in most glial cell genes for the hNS and 2-D protocols.

Chapter 4: Long Term Differentiation of Human Ventricular Cardiomyocytes

4.1 Abstract

Myocardial infarction (MI) is one of the leading causes of death in the United States. However, an effective treatment has yet to be developed that will allow for the repair of the damaged tissue leading to drastic loss in the heart efficiency. HPSC replacement therapies are thought to be a promising technique to allow for the regeneration of this damaged tissue. The development of a protocol that will allow for the scalable and efficient differentiation of hPSCs to ventricular cardiomyocytes (VCMs), the key damaged cell type of the heart, remains elusive. Here, I demonstrate that allowing VCMs to develop from cardiomyocytes through by temporal factors is an ineffective means of VCM differentiation.

4.2 Introduction

Cardiovascular disease currently affects more than 83.6 million Americans and is the leading cause of death in the United States. Out of those, 7.6 million have experienced a myocardial infarction (MI) (Go et al, 2013). An MI can cause the death of over 1 billion ventricular cardiomyocytes (VCMs), severally hampering the hearts ability to pump blood (Murry et al, 2006). The heart's capacity to repair itself is extremely limited, leading to the formation of scar tissue and loss of function of the cardiomyocyte (CM) tissue. To address this problem many groups are looking at hPSCs replacement therapies to regenerate the damaged muscle of the heart (Mariann et al, 2016). Directing

hPSCs to VCMs currently remains an inefficient process (Vincent et al, 2009). Here, I demonstrate that allowing VCMs to develop from cardiomyocytes through by temporal factors is an ineffective means of VCM differentiation.

4.3 Materials and Methods

4.3.1 Cell Culturing

A hESC ventricular report line was chosen for this experiment. MLC2V, a ventricular specific marker, was stably transfected with a GFP reporter allowing for the expression of GFP when MLC2V actively being expressed (Figure 4-1). GFP expression allowed for the visualization and counting via flow cytometry of VCMs of the time course of the experiment.

MLC2V-GFP were expanded and maintained in an undifferentiated state at standard conditions on Geltrex coated polystyrene tissue culture plates. Fresh E8 media was exchanged every day. Cells were allowed to grow till 70-80% confluent and were passed at 2×10^4 cells/cm^2, every three to four days as required.

4.3.2 Differentiation of hESCs to Cardiomyocytes

Once MLC2V reached 70-80% confluency media was changed to RPMI/B27 without insulin supplemented with 12 uM CHIR99021, a GSK-3 inhibitor that activates WNT signaling. Media was changed to RPMI/B27 without insulin 24 hours later. After 48 hours the media was exchanged for RPMI/B27 without insulin supplemented with 5 uM IWP2, a PORCN inhibitor leading to the inhibition of endogenous WNT processing and secretion. After 48 hours, media was exchanged for RPMI/B27 without insulin and then fresh RPMI/B27 without insulin was every three days.

4.3.3 Flow Cytometry

Flow cytometry was performed to analyze the percent of cells that were GFP^+. Every five days, cells were dissociated to single cell using typeLE (Life Technologies) and filtered through a 40 um cell strainer (Bio express) to remove cells clumps. They were then washed with FACS stain buffer (BD Bioscience) and run counted using a flow cytometer.

4.3.4 Statistical Analysis

All values are shown as mean ± standard deviation. A p-value of <0.05 was considered statistically significant.

4.4 Results and Discussion

The protocol for cardiomyocyte differentiation is extremely sensitive to cell density. Before a time course could be run several density gradients were performed (50%, 60%, 70%, 80, 90%, and 100% confluency) to determine optimal starting cell density (data not shown). Ideal differentiation starting confluency was determined to be between 70-80%.

Using the MLC2V-GFP reporter line, VCMs were measured using flow cytometry over the course of 80 days (Figure 4-3). Beating cardiomyocytes were present by day 8 in a majority of well with GFP expression starting on day 20 in a small population of cells (data not shown). There was a steady increase in GFP^+ cells between days 20 to 30. However, the GFP^+ expression leveled off with no significant increases from days 35 to 80. This demonstrates that there is a small temporal element in the

differentiation of hPSCs to VCMs. A majority of the cells remained either atrial or nodal cardiomyocytes.

4.5 Conclusion

In order for a heart failure cell replacement therapy to be effective it must have an extremely high efficiency in the differentiation of VCMs. The method tried here shows a slight increase in the generation of VCMs by allowing the CMs to mature over time. However, this increase is not efficient enough to allow for the cell quantities needed for a cell replacement therapy. Many groups have found high proficient methods of generating VCMs through the use of small molecules during the differentiation process (Karakikes et al, 2014). It is possible that through a combination of small molecule-mediated differentiation with the addition of the temporal factors highly efficient VCMs methods can be developed.

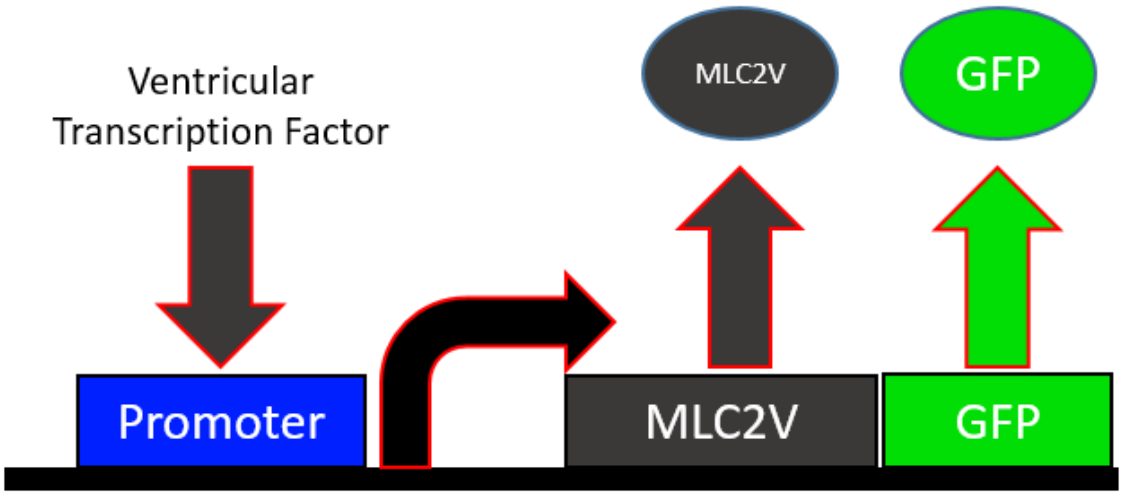

Figure 4-1: MLC2V GFP Reporter

The GFP reporter is directly downstream of the MLC2V gene. GFP is then expressed simultaneously with MLC2V when a ventricular transcription factor binds to the promoter region.

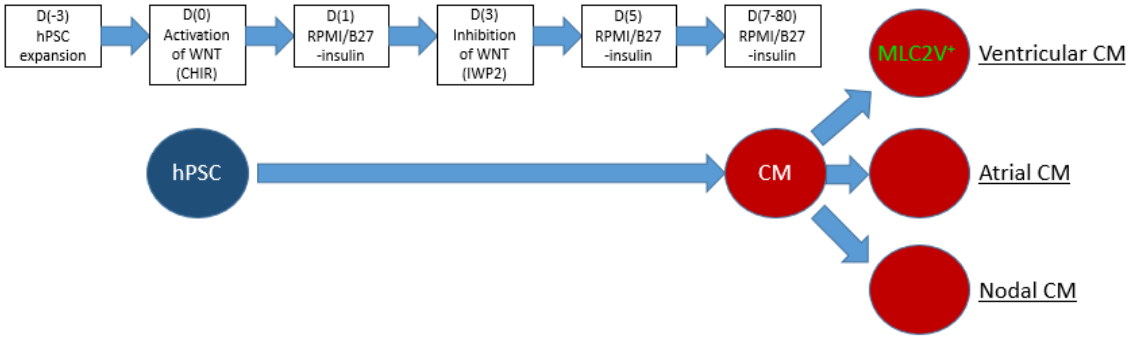

Figure 4-2: Ventricular Cardiomyocyte Differentiation Protocol

Protocol for cardiomyocyte differentiation. Over the course of seven days hPSCs are differentiated into cardiomyocytes (CM). These are then allowed to differentiate further into the three cell types of the heart: ventricular CMs, atrial CMs, and nodal CMs. This further differentiation us not directed by exogenous addition of small molecules or growth factors.

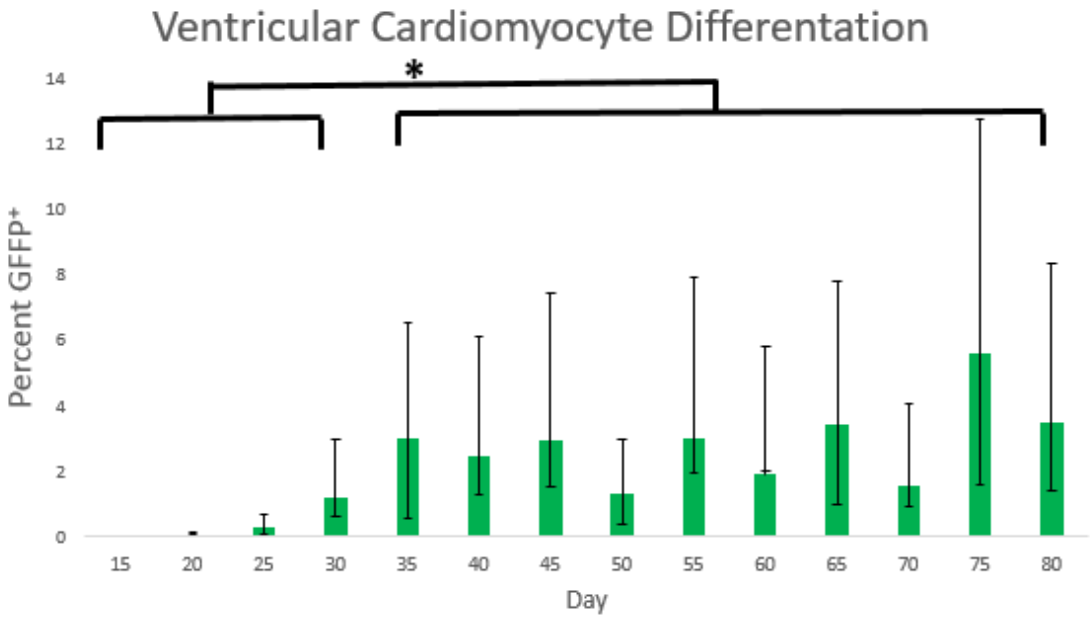

Figure 4-3: GFP Expression during Ventricular Cardiomyocyte Differentiation

Flow Cytometry for percent of GFP^+ cells that expressed the VCM marker, MCL2V. *P <0.05.

Chapter 5: Conclusions and Future Prospectives

5.1 Abstract

Throughout the course of the master's program I have developed and tested several differentiation methods as well as designed a panel of RT-qPCR primers for the analysis of the neuronal differentiation protocols. The 3-D neuronal protocols can be split into two categories: Matrigel™ and suspension. The 3-D Matrigel™ methods, thick and thin gels, proved as an unreliable method for neuronal differentiation. While still preliminary, the suspension culture neuronal differentiation of hNS demonstrated equivalent results of neuronal differentiation as standard 2-D methods, as analyzed using the panel of RT-qPCR primers. The cardiomyocyte differentiation showed limited capabilities in the production of VCMs over the course of 80 days. Here, I speculate as to the future of these projects and their potential use in their respective fields.

5.2 Developing A 3-D Neurodegenerative Disease *In Vitro* Model

To gain a greater understanding of neurodegenerative diseases, an *in vitro* model is needed that is able to recapitulate the many aspects of the disease pathophysiology. Therefore, the motivation for the hNS project is to develop a model which possess those capabilities. Currently, this project requires further optimization and analysis before it can be used as an effective method for neurodegenerative disease modeling. Once this has been achieved, the hNS can then be differentiated, through the use of neuronal patterning, to the many distinct neuronal subtypes (Moya et al, 2014). This would potentially allow for the study of diseases affecting the diverse areas of the brain.

The panel of RT-qPCR primers designed is a general panel useful in the analysis of unpatterned neuronal differentiation. To continue to be of use for the hNS project the panel needs to be expanded upon to include a larger variety of neuronal subtype specific primers. This would then allow for the examination of the patterned hNS. Once development and analysis of the hNS is completed, the in-depth study of many neurodegenerative diseases becomes possible.

5.3 Ventricular Cardiomyocyte Differentiation

Since ventricular muscle is the most detrimental to patient health when lost in a MI, it is critical that a protocol be developed for the efficient generation of VCMs for future cell replacement therapies. The method developed here demonstrated a temporal factor in the differentiation of VCMs. However, this factor is small, with only 2-6% of total cells expressing the ventricular marker, MLC2V. Currently, many groups are looking at the use of small molecules and growth factors to force the differentiation of hPSCs to VCMs (Karakikes et al, 2014). This is proving effective in the generation of a nearly pure population of VCMs with the addition of the temporal element.

5.4 Conclusion

The development of 3-D *in vitro* disease models will have significant impact in the study of neurodegenerative diseases by allowing for the recapitulation of the in-depth examination of the disease mechanisms. Furthermore, hNS could be used for the high-throughput drug screening by pharmaceutical companies in their attempt to find a treatment of these diseases. Here, I have emphasized the need for further optimization of the hNS protocol as well as the future uses of this system. It is my desire that this

protocol be used in the advancement of human knowledge and treatment of neurodegenerative diseases.

REFERENCES

Aarons, S, C Peisah and C Wijeratne. "Neuropsychiatric effects of Parkinson's disease treatment." *Australasian journal on ageing* 31 (2012): 198-202. Web.

Abbott, Alison, et al. "The Lure of Stem-Cell Lines." *Nature* 442 (2006): 336-337. Web.

Aggarwal, Anju and Shashiraj. "Juvenile amyotrophic lateral sclerosis." *The Indian Journal of Pediatrics* 73 (2006): 225-226. Web.

Andrews, Jinsy. "Amyotrophic lateral sclerosis: Clinical management and research update." *Current Neurology and Neuroscience Reports* 9 (2009): 59-68. Web.

Batalov, Ivan and Adam Feinberg. "Differentiation of Cardiomyocytes from Human Pluripotent Stem Cells Using Monolayer Culture." *Biomarker Insights* 10 (2015): 71-76. Web.

Benam, KH, et al. "Engineered in vitro disease models." *Annual Reivew of pathology* 10 (2015): 195-262. Web.

Blandini, F and MT Armentero. "Animal Models of Parkinson's Disease." *FEBS journal* 279 (2012): 1156-1166. Web.

Braak, H, et al. "Amyotrophic lateral sclerosis: dash-like accumulation of phosphorylated TDP-43 in somatodendritic and axonal compartments of somatomotor neurons of the lower brainstem and spinal cord." *Acta neuropathologica* 120 (2010): 67-74. Web.

Brafman, David. "Generation, Expansion, and Differentiation of Human Pluripotent Stem Cell (hPSC) Derived Neural Progenitor Cells (NPCs)." *Methods in Molecular Biology* 1212 (2015): 87-102. Web.

Brain Disorders: By the Numbers. 16 January 2014. Web. 15 Feburary 2016.

Brennand, K, et al. "Phenotypic differences in hiPSC NPCs derived from patients." *Molecular Psychiatry* 20 (2015): 361-368. Web.

Camille, Yvona, et al. "Using Stem Cells to Model Diseases of the Outer Retina." *Computational and Structural Biotechnology Journal* 13 (2015): 382-389. Web.

Castellani, R, R Rolston and M Smith. "Alzheimer Disease." *Disease-a-Month* 56 (2010): 484-546. Web.

Cave, JW, M Wang and H Baker. "Adult subventricular zone neural stem cells as a potential source of dopaminergic replacement neurons." *Frontiers in neuroscience* 8 (2014). Web.

Chambers, Stuart, et al. "Highly efficient neural conversion of human ES and iPS cells by dual inhibition of SMAD signaling." *Nature Biotechnology* 27 (2009): 275-280. Web.

Choi, S, et al. "A three-dimensional human neural cell culture model of Alzheimer's disease." *Nature* 515 (2014): 274-278. Web.

Damdimopoulou, Pauliina, et al. "Human Embryonic Stem Cells." *Clinical Obstetrics & Gynaecology* 31 (2016): 2-12. Web.

Desbordes, Sabrina and Studer Lorenz. "Adapting human pluripotent stem cells to high-throughput and high-content screening." *NATURE PROTOCOLS* (2013): 111-130. Web.

Feiler, M, et al. "TDP-43 is intercellularly transmitted across axon terminals." *The Journal of cell biology* 211 (2015): 897-911. Web.

Finkbeiner, Steven. "Huntington's Disease." *Cold Spring Harbor Perspectives in Biology* 3 (2011). Web.

Fisher, Elizabeth, et al. "New approaches for modelling sporadic genetic disease in the mouse." *Disease Models & Mechanisms* 2 (2009): 446-453. Web.

Frank, Samuel. "Treatment of Huntington's Disease." *Neurotherapeutics* 11 (2014): 154-160. Web.

Go, Alan and et al. "Heart Disease and Stroke Statistics 2013 Update." *Circulation* 127 (2013). Web.

Hartmann, Andreas. "Postmortem Studies in Parkinson's Disease." *Dialogues in Clinical Neurosecience* 6 (2004): 281-293. Web.

Huch, Meritxell and Boo-Kyoung Koo. *Modeling mouse and human development using organoid cultures*. 2015. <http://dev.biologists.org/content/142/18/3113>.

Jakel, Rebekah, Bernard Schneider and Svendsenm Clive. "Using human neural stem cells to model neurological disease." *Nature Reviews Genetics* 5 (2004): 136-144. Web.

Jiang, Zhengping, Yanmei Han and Xuetao Cao. "Induced pluripotent stem cell (iPSCs) and their application in immunotherapy." *Cellular & Molecular Immunology* 11 (2013): 17-24. Web.

Jones, Deryk. "Bioethics in Practice: A Quarterly Column About Medical Ethics: Stem Cell Ethics." *Ochsner Journal* 13 (2013): 8-10. Web.

Karagiannis, Peter and Shinya Yamanaka. "The Fate of Cell Reporgramming." *Nature Methods* 11 (2014): 1006-1008. Web.

Karakikes, Ioannis, et al. "Small Molecule-Mediated Directed Differentiation of Human Embryonic Stem Cells Toward Ventricular Cardiomyocytes." *Stem Cells Translational Medicine* 3 (2014): 18-31. Web.

Karran, E, M Mercken and B De Strooper. "The amyloid cascade hypothesis for Alzheimer's disease: an appraisal for the development of therapeutics." *Nature Reviews. Drug Discovery* 10 (2011): 698-712. Web.

Kim, Young Hye, et al. "A 3D human neural cell culture system for modeling Alzheimer's disease." *Nature Protocols* 10 (2015): 985-1006. Web.

Klein, C and A Westenberger. "Genetics of Parkinson's Disease." *Cold Spring Harbor Perspectives in Medicine* 2 (2012). Web.

Kowalski, Peter, et al. "Huntington's Disease." *Biological Perspectives* 51 (2015): 157-161. Web.

LaFerla, Frank and Kim Green. "Animal Models of Alzheimer Disease." *Cold Spring Harbor Perspectives in Medicine* 2 (2012). Web.

Lee, Yee-Ki, et al. "Efficient attenuation of Friedreich's ataxia (FRDA) cardiomyopathy by modulation of iron homeostasis-human induced pluripotent stem cell (hiPSC) as a drug screening platform for FRDA ☆." *International Journal of Cardiology* 203 (2016): 964-971. Web.

Lopez-Bayghen, Esther and Arturo Ortega. "Glial Glutamate Transporters: New Actors in Brain Signaling." *Life* 63 (2011): 816-823. Web.

Ludolph, AC, J Brettschnedier and JH Weishaupt. "Amyotrophic lateral sclerosis." *Current opinion in neurology* 25 (2012): 530-535. Web.

Makoto, Honda, et al. "The modeling of Alzheimer's disease by the overexpression of mutant Presenilin 1 in human embryonic stem cells." *Biochemical and Biophysical Research Communications* 469 (2016): 587-592. Web.

Mariann, Gyongyosi, et al. "Meta-Analyses of Human Cell-Based Cardiac Regeneration Therapies: Controversies in Meta-Analyses Results on Cardiac Cell-Based Regenerative Studies." *Circulation Research* 118 (2016): 1254-1263. Web.

Marino, Julie, Peyton Cook and Kenton Miller. "Accurate and statistically verified quantification of relative mRNA abundances using SYBR Green I and real-time RT-PCR." *Journal of Immunological Methods* 28. (2003): 291-306. Web.

McGonigle, P and B Ruggeri. "Animal models of human disease: challenges in enabling translation." *Biochemical Pharmacology* 87 (2014): 162-171. Web.

Miller, Justine, et al. "Human iPSC-Based Modeling of Late-Onset Disease." *Cell Stem Cell* 13 (2013): 697-705. Web.

Moore, D, et al. "Molecular pathophysiology of Parkinson's disease." *Annual review of neuroscience* 28 (2005): 57-87. Web.

Moya, Noel, et al. "Endogenous WNT Signaling Regulates hPSC-Derived Neural Progenitor Cell." *Stem Cell Reports* 3 (2014): 1015-1028. Web.

Murry, Charles, Hans Reinecke and Lil Pabon. "Regeneration Gaps : Observations on Stem Cells and Cardiac Repair." *Journal of the American College of Cardiology* 47 (2006): 1777-1785. Web.

Nakano, Imaharu. "Frontotemporal dementia with motor neuron disease (amyotrophic lateral sclerosis with dementia)." *Neuropathology* 20 (2001): 68-75. Web.

Noble, Wendy and Mark Burns. "Challenges in Neurodegeneration Research." *Frontiers in Psychiatry* 1 (2010). Web.

Novak, Marianne and Sarah Tabrizi. "Huntington's Disease." *BMJ* 341 (2010): 34-40. Web.

Oddo, S, et al. "Triple-transgenic model of Alzheimer's disease with plaques and tangles: intracellular Abeta and synaptic dysfunction." *Neuron* 39 (2003): 409-421. Web.

Orsini, Marco, et al. "Amyotrophic Lateral Sclerosis: New Perpectives and Update." *Neurology international* 7 (2015). Web.

Pandey, Ghanshyam and Yogesh Dwivedi. "What can Post-Mortem Studies Tell Us About the Pathoetiology of Sucide." *Future Neurol.* 5 (2010): 701-720. Web.

Pasca, Anca, et al. "Functional cortical neurons and astrocytes from human pluripotent stem cells in 3D culture." *Nature Methods* 12 (2015): 671-678. Web.

Patterson, Christopher, et al. "Diagnosis and treatment of dementia: 1. Risk assessment and primary prevention of Alzheimer disease." *CMAJ* 178 (2008): 548-556. Web.

Politis, M and O Lindvall. "Clinical application of stem cell therapy in Parkinson's disease." *BMC Med* 10 (2012). Web.

Pratt, AJ, ED Getzoff and JJ Perry. "Amyotrophic lateral sclerosis: update and new developments." *Degenerative neurological and neuromuscular disease* 2 (2012): 1-14. 2012.

Prince, M, et al. "The global prevalence of dementia: a systematic review and metaanalysis." *Alzheimers Dementia* 1 (2013): 63-75. Web.

Pringsheim, T, et al. "The prevalence of Parkinson's disease: a systematic review and meta-analysis." *Mov Disord* 29 (2014): 1583-1590. Web.

"Real-Time PCR Hanbook." 2016. *Theromfisher.com.* Web. 17 April 2016.

Ring, Karen. *CIRM-Funded Study Suggests Methods to make Pluripotenet Stem Cells are Safe*. 22 February 2016. Web. 2 April 2016.

Rippon, H and A Bishop. "Embryonic Stem Cells." *Cell Proliferation* 37 (2004): 23-34. Web.

Sanchez-Danes, A, et al. "Induced Pluripotent Stem Cell-Based Studies of Parkinson's Disease: Challenges and Promises." *CNS Neurological disorders drug targets* 12 (2013): 1114-1127. Web.

Schapira, A. "Neurobiology and Treatment of Parkinson's Disease." *Trends in Pharmacological Sciences* 30 (2009): 41-47. Web.

Segers, VF and RT Lee. "Stem-Cell Therapy for Cardiac Disease." *Nature* 451 (2008): 937-942. Web.

Sharon, Paige, et al. "Molecular Regulation of Cardiomyocyte Differentiation." *Circulation Research* 116 (2015): 341-353. Web.

Simmons, Danielle. "The Use of Animal Models in Studying Genetic Disease: Transgenesis and Induced Mutation." *Nature Education* 1 (2008). Web.

Stem Cell Basics. 05 March 2015. Web. 2 March 2016. <http://stemcells.nih.gov/info/basics/pages/basics1.aspx>.

Stem Cells 1. n.d. Web. 30 March 2016. <https://infograph.venngage.com/p/57961/stem-cells-1>.

Sterneckert, Jared, Peter Reinhardt and Hans Scholer. "Investigating human disease using stem cell models." *Nature Reviews Genetics* 15 (2014): 625-639. Web.

Sung, Kyung Eun, et al. "Understanding the Impact of 2D and 3D Fibroblast Cultures on In Vitro Breast Cancer Models." *PLOS One* 8 (2013). Web.

Takahashi, Kazutoshi, et al. "Induction of Pluripotent Stem Cells from Adult Human Fibroblasts by Defined Factors." *Cell* 131 (2007): 861-872. Web.

Takanashi, K and A Yamaguchi. "Aggregation of ALS-linked FUS mutant sequesters RNA binding proteins and impairs RNA granules formation." *Biochemical and biophysical research communications* 452 (2014): 600-607. Web.

Tischa, van der Cammen, et al. "Genetic Testing Has No Place as a Routine Diagnostic Test in Sporadic and Familial Cases of Alzheimer's Disease." *Jounral of American Geriatrics Society* 52 (2004): 2110-2113. Web.

Vats, A, et al. "Stem Cells." *Lancet* 366 (2005): 592-602. Web.

Vincent, Huei-Sheng, Changsung Kim and Mercola Mark. "Electrophysiological Challenges of Cell-Based Myocardial Repair." *Circulation* 120 (2009): 2496-2508. Web.

Wu, T and M Hallett. "The cerebellum in Parkinson's disease." *Brain* 136 (2013): 696-709. Web.

Yagi, Takua, et al. "Modeling Familial Alzheimer's Disease With Induced Pluripotent Stem Cells." *Juman Molecular Genetics* 20 (2011): 4530-4539. Web.

Yarnall, Alison, Neil Archibald and David Burn. "Parkinson's Disease." *Medicine* 40 (2012): 529-535. Web.

Ye, Jianl, et al. "Primer-BLAST: A tool to design target-specific." *Bioinformatics* 13 (2012). Web.

Yitshak, Sade, et al. "Parkinson's Disease Prevalence and Proximity to Agricultural Cultivated Fields." *Parkinson's disease* 18 (2015): 567-576. Web.

APPENDIX A

TABLE 1: FORWARD AND REVERSE PRIMERS USED FOR RT-QPCR

Gene	Forward	Reverse	Product Length (bP)
NPC			
SOX1	AATACTGGAGACGAACGCCG	CCCTCGAGCAAAGAAAACGC	182
SOX2	GCGGAAAACCAAGACGCTCA	TCATGCTGTAGCTGCCGTTG	123
NESTIN	CGCACCTCAAGATGTCCCTC	CAGCTTGGGGTCCTGAAAGC	128
Neuronal			
B3T			
MAPT	AGGGGGCTGATGGTAAAACG	TTGCTTAGTCGCAGAGCTGG	140
NCAM1	GATGCGACCATCCACCTCAA	CCAGAGTCTTTTCTTCGCTGC	178
Neuronal Subtype			
ACHE	CACAGGGGATCCCAATGAGC	CGTCGAGCGTGTCGGTG	18
SLC6A4	AGAATTTTACACGCGCCACG	GAGGTCTTGACGCCTTTCCA	
EAAT3	TGGTGCTAGGCATTACCACA	CCGGATACGTTGGAATCCAGT	172
GABRA1	TGCGGATTTCGTCCTGACTT	AATCTGCAGCTCTGAATTGTGC	194
GRIN2A	AGCCTCCGGCTGGGATAG	CCACTGACGGTCCCTGTAG	191
Glial			
EAAT2	ATGGCATCAACAGAGGGTGC	CTCCCAGGATGACACCAAACA	172
GFAP	AACCTGCAGATTCGAGGGGG	GGCGGCGTTCCATTTACAATC	128
MBP	CTGTGCAACATGTACAAGGACTC	GGGACAGTCCTCTCCCCTTT	175
S100B	GGGAGACAAGCACAAGCTGA	CCTCCTGCTCTTTGATTTCCTCTA	91

APPENDIX B

TABLE 2: NPC, NEURAL, AND GLIAL RT-QPCR PRIMERS DESIGNED AND VALIDATED

Gene Abbreviation	Gene Name	Summary
SOX1	SRY- Box 1	Pluripotency marker
SOX2	SRY- Box 2	NPC marker
NESTIN	Nestin	Neuron intermediate filament protein
B3T	Tubulin, Beta 3 Class III	Neuron microtubule protein
MAP2	Microtubule-Associated Protein 2	Neuron microtubule assembly
MAPT	Microtubule-Associated Protein Tau	Neuron microtubule assembly and stability
ACHE	Acetylcholinesterase	Hydrolyzes ACH in brain
SLC6A4	Solute Carrier Family 6, Member 4	Serotonin neurotransmitter membrane protein
EAAT3	Solute Carrier Family 1, Member 1	Glutamate neurotransmitter membrane protein
GABRA1	Gamma-Aminobutyric Acid A Receptor, Alpha 1	GABA neurotransmitter receptor
GRIN2A	Glutamate Receptor, Innotropic, N0Methyl D-Asparate 2A	Glutamate-gated ion channel
NCAM1	Neural Cell Adhesion Molecule 1	Neuron development
S100B	S100 Calcium Binding Protein B	Astrocytosis
EAAT2	Solute Carrier Family 1	Glial glutamate transporter
GFAP	Glial Fibrillary Acidic Protein	Mature astrocyte intermediate filament
MBP	Myelin Basic Protein	Constituent of myelin sheath of oligodendrocyte